Suppression of Torsional Oscillations in a High-Performance Speed Servo Drive

Slobodan N. Vukosavić, *Member, IEEE*, and Milić R. Stojić, *Associate Member, IEEE*

Abstract— This paper deals with the problem of mechanical resonance in modern servo drive systems having the speed control loop bandwidth and resonance frequency above 100 Hz. To enable the extension of the range of stable gains in the presence of flexible coupling, a simple and straightforward modification of the speed loop controller is proposed in order to augment the performance of present speed controllers and to make them accordant with mechanical structure suffering from the compliance problem. This paper is comprised of the analytical considerations, straightforward design guidelines, and results of experimental verification obtained by an experimental setup with the elastically coupled 7-N·m synchronous servo motor and mechanical resonance frequency of 160 Hz.

Index Terms— Finite-duration impulse-response digital filter, motor drive, resonance, rotating machine mechanical factors, velocity control.

I. INTRODUCTION

SERVO DRIVES in modern machining centers fulfill the task of moving, with high dynamics and accuracy, machine parts along prescribed tracks. The bandwidth of a speed control loop required by numerically controlled (NC) machine tools, punching, water- and laser-cutting machines exceeds 100–200 Hz. Elastic couplings and joints within the system plant are major impediments to the performance enhancement, since high loop gains often destabilize torsional resonance modes associated with the transmission flexibility.

Servo motors in a typical industrial environment are linked to their end effectuators by transmission mechanisms having a finite stiffness. The elastically coupled two-mass motor/load system introduces finite zeros and the pair of conjugate complex poles in the transfer function of the system plant and, thus, brings up the problem of mechanical resonance. The problem is more emphasized in servo systems with position feedback sensors attached to the load side, e.g., to the end effectuator. Then, the closed loop will encompass unmodeled torsional resonance modes. The same resonance phenomenon appears in servo systems with a feedback sensor attached to the motor shaft. In such a case, the range of stable loop gains is severely limited, along with the overall drive performance. Moreover, the load impact or the reference step input may provoke weakly damped oscillations of the link.

A typical brushless dc servo actuator with an infinite inertia load stiffly connected to the rotor shaft has an inherent resonance frequency ranging from 500 Hz to 2 kHz. Rarely used as direct drives, motors are mostly coupled through reduction gears allowing the usage of high-speed high-power-to-weight-ratio motors. The compliance is especially noticeable in the case of toothed-belt-transmission and harmonic drives. Such a coupling might have the stiffness coefficient of a lower value. Even with a low rotor inertia of high specific power motors, such a stiffness may result in mechanical resonance frequencies ranging from 30 to 300 Hz. Often ignored in designing conventional servo systems, such resonance modes might overlap with the bandwidth of the speed control loop and cause sustained oscillations of the machine links and parts. This behavior is often perceived as an audible "humming" of the system caused by 100–300-Hz oscillations of the system parts and masses. The noise is accompanied by excessive torque/force oscillations that might damage joints and parts. Besides the metal fatigue, parasitic oscillations leave their signature on the work piece in the case of machine tools and wood-working, laser- and water-cutting machines.

High servo loop gains are required to decrease the error in tracking of fast and steep trajectories. Nevertheless, high control loop gains cannot be used, due to mechanical resonance modes frequently encountered as unmodeled dynamics within the servo system plant. This paper provides means of improving the robustness of existing servo loop controllers with respect to torsional resonance, enabling a significant increase of stable control loop gains.

In the field of industrial drives, the torsional resonance problems were encountered first in rolling mill applications [1]–[3], [12], [13]. Long shafts and large inertia constitute a weakly damped mechanical resonator exhibiting a relatively low (10–20 Hz) resonance frequency. Vibrations caused by the load impact and the step input endanger the integrity of the mechanical structure and deteriorate the product quality. Most drive systems possess a single feedback device and oscillatory mechanical subsystem with states that are generally unmeasurable. For that reason, the suppression of mechanical vibrations is a control problem that attracted the attention of many researchers over the past decade. Solutions being proposed may be divided into the following three groups: 1) control strategies based on the direct measurement of motor- and load-side variables [15], [22], [24]; 2) strategies involving only one feedback device attached to the motor and the observer that estimates remaining states [2]–[4], [8], [10], [12], [13]; and 3) vibration suppression strategies based upon the notch filtering and phase-lead compensation applied in conventional speed control structures [4], [16], [17], [23].

Meschkat [23] proposed the increase of the stability margin by means of the phase-lead compensator or by using notch filters with the center frequency set to cancel the resonance modes. The desired damping of the system may be provided by augmenting the driving force using the first derivative of the load torque [1], [4], [16]. To this end, Ohmae [1] proposed the hardware-implemented load torque observer. The phase-lead compensation with software-implemented observer has been proposed by Sugiura [4].

The problem of mechanical oscillations is alleviated by a simulator following control [5], [6]. An excitation brought to resonance modes might be reduced by imposing the acceleration control loop [7], [21]. For that purpose, it is necessary to observe and control the load-side acceleration. The removal of sudden jumps in the electromagnetic torque, i.e., limiting the motor side acceleration, excludes the excitation of resonance modes coming from the motor side. In this case, the mechanical resonator is excited by the load impact only. Although efficient, a slow change of the reference input severely limits the overall performance of the drive.

The desired damping is obtained by adding a control term proportional to the speed difference [15], [17], [22], which requires measurements of both the motor and load velocities. The application of two shaft sensors is impractical in an industrial environment and, therefore, many authors suggested that the shaft torque and load speed be obtained by means of the state observer [2], [3], [12], [13].

State controllers with pole assignment and linear-quadratic-regulator (LQR)-based parameter setting require all states of the oscillatory mechanical subsystem to be known with sufficient accuracy, noise free, and with short delay times. Ji [10] proposed the Kalman state estimator to improve the state estimation, assuming that disturbances and sensor imperfections might be modeled by the white noise.

A typical machine tools set is comprised of brushless dc motors with a one-per-axis shaft sensor integrated with the motor. The shaft sensor is usually the electromagnetic resolver with resolver-to-digital (R/D) converter or the optical encoder. State observers using signals from these sensors are severely limited in their performances as the frequency range of interest increases above 100 Hz. Moreover, finite resolutions of such sensors restrict the state estimation process [1], in particular at low speeds. On the other hand, resolvers have intrinsic errors related to the number of sensing device poles and slots, errors caused by the R/D converter imperfections [18]–[20], and synthesized resolution that drops down to 10 b for high-speed axis and spindle drives. An R/D converter may be treated as a hardware-implemented closed-loop observer with 1-kHz cutoff frequency [20] and typical transport lag of 500 μs. Applied in an industrial environment, shaft transducers (optical encoders and electromagnetic resolvers) exhibit limited bandwidths and relatively low resolutions. The noise-contaminating detected signals do not have the properties of the Gaussian noise; rather, it contains both components related to the pulsewidth modulation (PWM) frequency of the drive amplifier and variable-frequency components related to the motor speed, number of motor and resolver poles, and resolver excitation frequency. Thus, state variables of a mechanical subsystem can
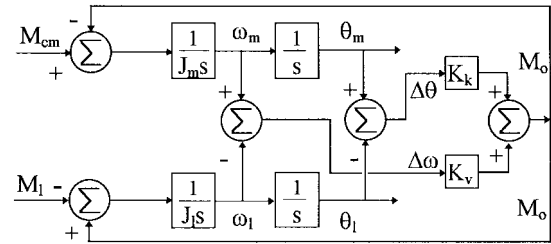

Fig. 1. Block diagram of the servo system with flexible coupling.

be estimated from detected signals with a limited bandwidth and relatively large transport lags that are inappropriate for suppressing unwanted mechanical oscillations above 100 Hz.

We improve the existing control structures and motion control algorithms to make them compatible with the mechanical subsystem. Note that many controllers already exist in the field, but all of them are designed by assuming an ideal, rigid transmission train. Due to the high specific power, low inertia motors, and elastic (toothed belt-like) transmission, the suggested controllers exhibit low dynamic performances. Specifically, high loop gains required for the desired speed of system response cannot be applied because they provoke the mechanical resonance phenomena. We propose a simple software-implemented filtering structure, which extends the range of applicable gains that significantly enhance servo performances. The proposed structure is intended for high-performance servo drives where the relevant frequency range and the imperfection of shaft sensors [18]–[20] prevent the estimation of unmeasured states. The antiresonant feature of the structure is not based on the exact cancellation of resonance poles. In Section IV, the robustness of the structure with respect to mechanical parameters uncertainty is verified by an experimental setup.

II. SERVO SYSTEM WITH ELASTIC DRIVE TRAIN

Fig. 1 shows the schematic diagram of a two-mass motor/load system with flexible coupling. In Fig. 1, electromagnetic torque M_{em} is obtained at the output of the speed controller. The motor inertia J_m and load inertia J_l are coupled by the shaft or the transmission system having a finite stiffness coefficient K_s. A flexible coupling doubles the number of state variables within the mechanical subsystem of the drive. Generally, the speed ω_m and position θ_m of the motor shaft differ from the respective variables ω_l and θ_l on the load side. The two-mass $J_m - K_s - J_l$ system is damped mainly by the viscous friction $K_v \Delta \omega$. The friction coefficient K_v generally assumes very low values, giving rise to weakly damped mechanical oscillations. The torsional torque M_o equals the load torque M_l only in the steady state. During transients, the speeds of motor and load differ, and torsional torque M_o is given by

$$M_o = K_s \Delta \theta + K_v \Delta \omega. \qquad (1)$$

Transfer function $W_m(s) = \omega_{\text{out}}(s)/M_{em}(s)$ of the mechanical subsystem differs from the simple $1/Js$. If the shaft
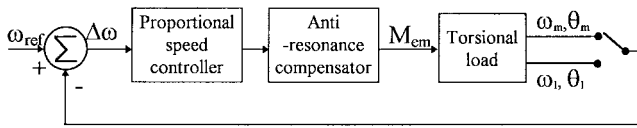
Fig. 2. Speed controller with the proportional action and torsional load.

sensor is mounted on the motor, $W_m(s)$ is defined by

$$W_m(s) = \frac{1}{(J_m + J_l)s} \frac{1 + \dfrac{K_v}{K_s}s + \dfrac{J_l}{K_s}s^2}{1 + \dfrac{K_v}{K_s}s + \dfrac{J_l J_m}{K_s(J_m + J_l)}s^2}$$

$$= \frac{1}{(J_m + J_l)s} \frac{1 + \dfrac{2\zeta_z}{\omega_z}s + \dfrac{1}{\omega_z^2}s^2}{1 + \dfrac{2\zeta_p}{\omega_p}s + \dfrac{1}{\omega_p^2}s^2}. \tag{2}$$

For systems where the shaft sensor detects load variables ω_l and θ_l at the end effectuator, the mechanical subsystem of the drive has the transfer function $W_l(s)$ given by

$$W_l(s) = \frac{1}{(J_m + J_l)s} \frac{1 + \dfrac{K_v}{K_s}s}{1 + \dfrac{K_v}{K_s}s + \dfrac{J_l J_m}{K_s(J_m + J_l)}s^2}$$

$$= \frac{1}{(J_m + J_l)s} \frac{1 + \dfrac{2\zeta_z}{\omega_z}}{1 + \dfrac{2\zeta_p}{\omega_p}s + \dfrac{1}{\omega_p^2}x^2}. \tag{3}$$

In (2) and (3), undamped natural frequencies (ω_p, ω_z) and relative damping coefficients (ζ_p, ζ_z) are given by

$$\omega_p = \sqrt{\frac{K_s(J_m + J_l)}{J_m J_l}}, \quad \omega_z = \sqrt{\frac{K_s}{J_l}}$$

$$\zeta_p = \sqrt{\frac{K_v^2(J_m + J_l)}{4K_s J_m J_l}}, \quad \zeta_z = \sqrt{\frac{K_v^2}{4K_s J_l}}. \tag{4}$$

The effect of flexible coupling on the closed-loop performance of the drive is strongly influenced by the location of the feedback transducer. Fig. 2 shows the block diagram of a simple proportional speed controller applied to the motor with torsional load. The block diagram indicates the possibilities of closing the control loop by using either motor- or load-side feedback and application of a cascade compensator that cancels or mediates unwanted resonance modes associated with a flexible mechanical subsystem. In the later analysis, related to the structure in Fig. 2, the drive system is considered ideal, except for the time lag caused by the speed calculation, control algorithm execution, and dynamics of the stator current controller.

A. Speed Control Loop with Motor Feedback

Undamped natural frequencies ω_p and ω_z of the pole- and zero-pairs in (2) are referred to as the resonance and antiresonance frequencies [4], and their quotient is known as
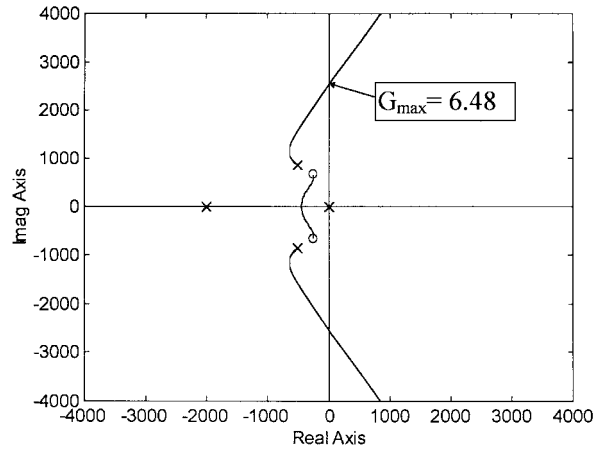
(a)
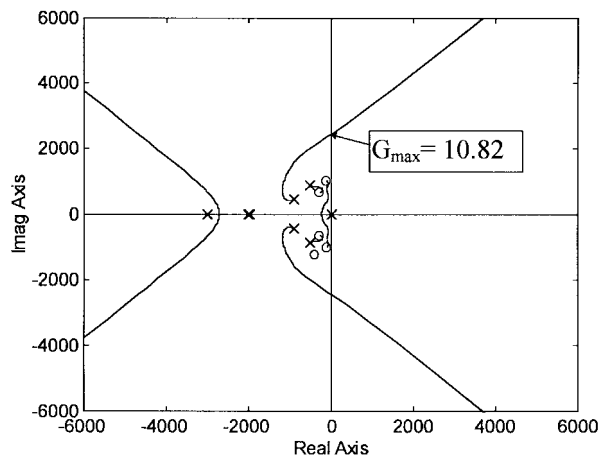
(b)

Fig. 3. Root locus illustrating the gain limits due to the presence of torsional load. (a) Noncompensated speed servo with proportional gain and the sensor attached to the motor. (b) Compensated speed servo with the proportional gain and the sensor attached to the motor. The series notch filter compensator has the damping coefficient mismatch of 0.5/0.1. The double pole at 2000 rad/s models the total lag within the current controller and the R/D converter.

the resonance ratio

$$R_r = \frac{\omega_p}{\omega_z} = \sqrt{1 + \frac{J_l}{J_m}}. \tag{5}$$

Attached to the motor, the sensor provides correct motor speed signal; that is, the motor-load compliance does not deteriorate measurement of the motor speed and position. Hence, the mechanical resonator is not enclosed in the control loop. An insight to the effects of such coupling is obtained by deriving the closed-loop poles of the simplified system (Fig. 1) with the proportional speed controller and the sensor on the motor shaft. To this end, it is assumed that the resonant frequency equals $\omega_p = 1000$ rad/s with the resonance ratio of $R_r = 1.41$ and the damping of $\zeta_p = 0.5$. From the root locus in Fig. 3(a), one can see that the unwanted coupling limits the range of stable gains. In the case under consideration, a low value of resonance ratio reduces the influence of torsional load on the dynamics of the speed control loop. With $J_m \gg J_l$, oscillations of torsional torque are filtered by a large motor inertia J_m and their influence on the control of the motor speed becomes smaller. With R_r close to unity, the complex

poles and zeros in Fig. 3(a) will form doublets that should cancel each other for $R_r = 1$.

Nevertheless, the case $J_m \gg J_l$ with resonance ratio R_r close to unity is most critical as far as the performance in control of the load-side variables is concerned. Precisely, a damped control of θ_m and ω_m is favorable, but most applications require fast and precise control of the end effectuator and the load variables θ_l and ω_l. Since a large motor inertia ($J_m \gg J_l$) impedes the penetration of torsional oscillations from the load to the motor, the estimation of resonance modes from detected signals (θ_m and ω_m) is not feasible. Actually, the motor speed ω_m contains information on remote states (θ_l and ω_l) of the mechanical subsystem, although in an amount commensurable with the ratio J_l/J_m. Moreover, in the case of $J_m \gg J_l$, secondary effects (the noise and sensor imperfection) exclude the possibility of applying an observer of load-side states. Therefore, even with a stiff and rigid control over ω_m, the load speed and position might exhibit weakly damped oscillations that cannot be disclosed and compensated for from the feedback signals.

The active cancellation of resonance modes may be accomplished by the state feedback [9]–[14]. The resonance behavior is suppressed by adjusting closed-loop poles through the pole assignment method or the implementation of LQR. In doing so, the undamped natural frequency of critical poles remain unchanged, but the relative damping coefficient is increased by rotating their radius toward the real axis. The state feedback approach offers the possibility of achieving arbitrary dynamics, but its application is troublesome, requiring remote states (θ_l and ω_l) be known with short delay times and a sufficient precision. The torsional torque M_o may be determined by means of an estimator [4], supposing that the rotor inertia J_m is known and that the frictional torque (i.e., mechanical loss within the motor) is negligible:

$$M_o = M_{em} - J_m \frac{d}{dt}\omega_m = M_{em} - J_m \frac{d^2}{dt^2}\theta_m. \qquad (6)$$

An introduction of a new driving force term [4] proportional to the first derivative of M_o may stabilize both the two-mass and three-mass mechanical subsystems. Due to the noise contained in the shaft sensor signals, Sugiura [4] proposed "softened" differentiators (e.g., differentiators fitted out with low-pass filters) within the estimator of M_o and in the proposed vibration-suppressing compensator.

The torque estimation through differentiation of the motor velocity has less chance of being successfully employed in servo drives with high cutoff frequencies. Specifically, the quantization noise [18], [19], repetitive error signals [19], [20], and R/D internal dynamics [20] highly contaminate the detected θ_m signal at the frequency band beyond 100 Hz. Bearing in mind that compensation based on (6) effectively implies triple differentiation of detected position (i.e., $d^3(\theta_m)/dt^3$), it is obvious that the elevated noise level may be suppressed only by heavy low-pass filters. Such filters deteriorate the phase characteristic and impede the vibration-suppressing action of the compensator: *The desired speed-loop bandwidth in modern machining centers approaches the frequency of torsional resonance and coincides, at the same time, with most disturbing statistical and deterministic noises.* An estimation of the torsional torque under the aforementioned conditions becomes difficult, and does not exact and sufficiently fast estimates.

Instead of using the estimator, inaccessible states and the torsional torque might be derived by the state observer. However, whatever the method of selecting observer gains, the bandwidth must include frequencies of unmodeled resonance modes. Thus, the noise-amplifying (derivative) nature of the observer extends over the entire frequency band of interest. Consequently, an observer-based acquisition of remote (θ_l and ω_l) states becomes problematic for the same reasons that prevent usage of an estimator (6).

Since the active compensation becomes impracticable in the case of a high resonance frequency, passive approaches such as the notch filter compensator were considered and proposed [23]. The task of increasing the relative damping coefficient of critical poles [Fig. 3(a)] might be accomplished by the cascade compensator with the notch filter. The notch filter zeros (7) are to cancel critical poles, while the poles of the filter become a new pair of conjugate complex poles with increased relative damping coefficient ($\zeta_p \gg \zeta_z$):

$$W_{\text{notch}} = \frac{s^2 + 2\zeta_z\omega_{NF}s + \omega_{NF}^2}{s^2 + 2\zeta_p\omega_{NF}s + \omega_{NF}^2}. \qquad (7)$$

In the mechanical subsystem, the equivalent inertia changes during each operating cycle, and the friction coefficient varies with the speed and machine wear. Hence, the exact location of critical poles is unknown and, thus, the cancellation is generally imprecise. Then, the resonance poles and the zeros of the notch filter will not coincide and pole–zero doublets will appear in the root locus. In Fig. 3(b), the root locus is given for the system of Fig. 2, compensated for with a series notch filter. It is assumed that the damping of filter zeros does not match the damping of critical poles. It may be observed that the notch compensation, even mismatched, significantly increases the range of stable gains.

B. Speed Loop with Load Feedback

The transfer function of the mechanical subsystem (Fig. 1) with the feedback sensor attached to the load is given by (3). Resonant modes are enclosed by the loop, since the speed feedback is derived from the position θ_l of the end effectuator or tool. Transfer function $W_l(s)$ in (3) differs from $W_m(s)$; instead of having a pair of finite complex zeros, function $W_l(s)$ has a single real zero at $z = -K_s/K_v$. Then, the applicable loop gain is found to be more than four times lower as the feedback device moves from the motor to the load. Nevertheless, the load-side feedback provides precise and compliance-free information on the position of the end effectuator. Providing stability conditions are reached, the tool will track the reference trajectory in spite of the twist $\Delta\theta$.

As in the previous case, a high-frequency mechanical resonance of the servo with load-side feedback can hardly be suppressed in an active way. The derivative nature of an estimator (6) or of a state observer makes the sensor noise overwhelm the information on unmeasurable states (M_o, ω_m, θ_m). Specif-
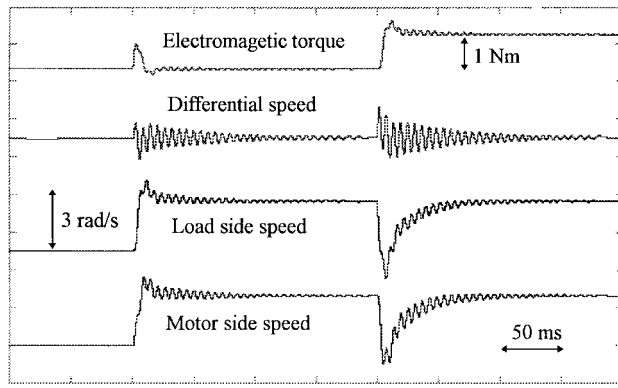
(a)
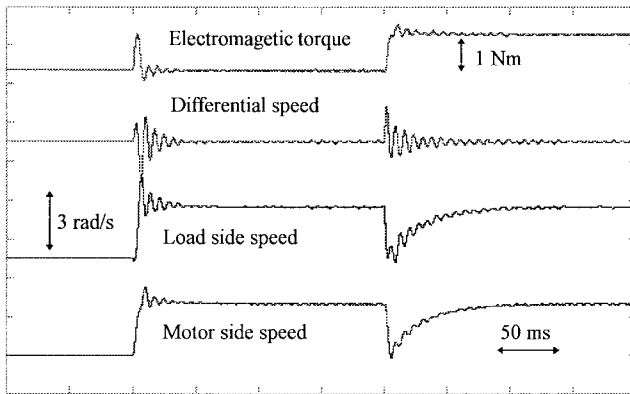
(b)

Fig. 4. Simulation traces of the reference step and the load step responses for elastically coupled servo with no series compensator with the relative gain of $G = 1.45$. (a) The system with motor-side feedback. (b) The system with load-side feedback.

ically, the spectral energy of statistical and deterministic parasitic signals coming from the shaft sensor [18]–[20] coincides or drops below mechanical resonance frequencies, making the state feedback approach inapplicable. The following section investigates the properties of the notch filter compensator by means of computer simulation of the system of Fig. 2. In Section III, a simpler and more robust compensator is proposed and tested as well.

III. SERIES NOTCH AND FINITE-DURATION IMPULSE-RESPONSE (FIR) FILTER COMPENSATOR

The dynamic behavior of the system with flexible coupling (Fig. 2) is investigated for both the motor-side and the load-side feedback, using the parameters and data listed in Appendix II. In Fig. 4(a), the load step response and the response to the step change of the reference speed are shown for the noncompensated speed controller based on the motor-side feedback. Both disturbances provoke weakly damped oscillations, visible in the "differential speed" trace, giving the difference between the motor and the load actual speeds.

The traces in Fig. 4(a) are repeated for the case of the load-side feedback, and the results are given in Fig. 4(b). Notice that resonance modes have slightly higher amplitudes and decline faster. In both simulations of a noncompensated
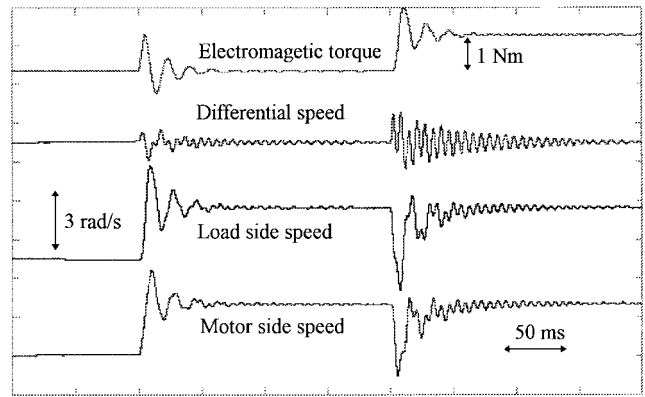

Fig. 5. Detuning of the notch compensator. The dynamic response with 25% detuning of the damping of the notch filter zero. The relative gain $G = 1.45$.

speed controller, the relative gain G is set to the maximum acceptable level.

The undamped natural frequency and relative damping coefficient of complex poles in transfer functions $W_l(s)$ and $W_m(s)$ [(2) and (3)] are $\omega_p = 992$ rad/s and $\zeta_p = 0.005$. The notch filter compensator is designed according with (7) and Appendix I. Its discrete version is connected in cascade with the speed controller, in order to suppress the resonance problems and to extend the range of stable gains. Filter zeros cancel the weakly damped poles of $W_m(s)$ and replace them with a complex pole pair with the relative damping coefficient of $\zeta_p = 0.005$.

For an exact cancellation of resonance modes, both the resonance frequency and damping factor (i.e., the coefficient of viscous friction) must be known while tuning five parameters of the notch filter (see Appendix I). The robustness of notch compensation with respect to a parameter mismatch has been examined by the simulation illustrated in Fig. 5. In simulation runs, an error amounting to 25% is assumed between the damping coefficient of the compensator zeros and the damping of related system poles. While the resonant frequency ω_p may be obtained off line or on line without major difficulties, the viscous friction is generally not known, and it presents a serious problem in tuning the notch compensator. Hence, a detuning of filter parameters $K1$–$K5$ (Appendix I) greatly reduces the positive effects of the compensator.

Therefore, we propose that the conceived cascade antiresonance compensator is simpler, less sensitive to parameter changes, and requiring a setting of only one parameter. This compensator is used instead of the notch filter of Fig. 2 to alleviate the torsional resonance problems in a passive way. The task imposed on the proposed series antiresonant compensator is, essentially, to filter the torque command signal. Ideally, all spectral components should remain unaltered, except those coinciding with the mechanical resonance frequencies of the drive train. Hence, the passive series compensator, by its nature, represents a bandstop filter. Consequently, as long as the driving torque has no spectral components at the resonance frequency, no energy is injected into the resonance modes. Specifically, an increase of the loop gain will not sustain the energy of the mechanical resonator and, thus, higher gains will
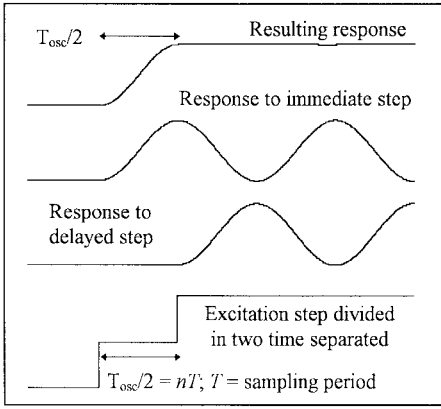
Fig. 6. The effects of the simplified FIR ($0.5 + 0.5\ z^{-n}$) filter on the response of undamped second-order system.
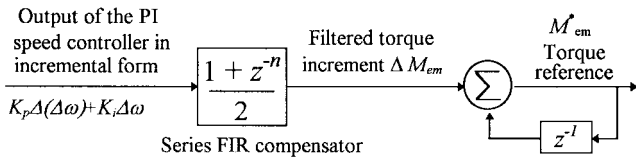

Fig. 7. Proposed series antiresonant compensator applied to the speed controller implemented in the incremental form.

be attainable, along with improvements in the performance of the speed control loop.

The notch filter suppresses the resonant frequency by the ratio ζ_p/ζ_z between the relative damping coefficients of the notch poles and zeros. Since a low damping coefficient of zeros increases greatly the sensitivity to parameter variations, the ratio ζ_p/ζ_z is limited. Hence, the excitation of resonance modes can be only reduced, but not eliminated completely, by the notch series compensator.

A simple way to fully suppress the excitation of resonance modes is illustrated in Fig. 6. The lowermost trace represents the excitation, i.e., the input to a second-order resonant plant. Such a step input provokes the undamped response of $1 - \cos(\omega t)$ type. As can be seen, the step input comprises two half steps at different time instants. If the time delay of the second half step is set to one-half period of the plant resonance frequency, oscillatory responses will have their pulsating components with opposite phases; consequently, pulsations nullify each other and the resulting response (the uppermost trace) becomes acceptable.

The incremental form of the speed controller is shown in Fig. 7. The controller accumulates increments of proportional and integral actions $\Delta M_{em} = K_p\Delta(\Delta\omega) + K_i\Delta\omega$ into resulting value M_{em} of the driving force. Interpreting each increment ΔM_{em} as the step trace in Fig. 6, it is perceivable that the excitation of resonance modes might be excluded by splitting each increment into two equal half steps, the later one being delayed by one-half of resonance period T_{osc}. The series compensator in Fig. 7 is essentially a digital FIR bandstop filter. The theoretical value of the suppression at $\omega_{ocs} = 1/T_{osc}$ frequency is infinite, rather than a finite ζ_p/ζ_z notch filter suppression value. Besides slightly better phase characteristics, the proposed form of FIR series compensator requires only one parameter (delay time $T_{osc}/2$) to be known and set.
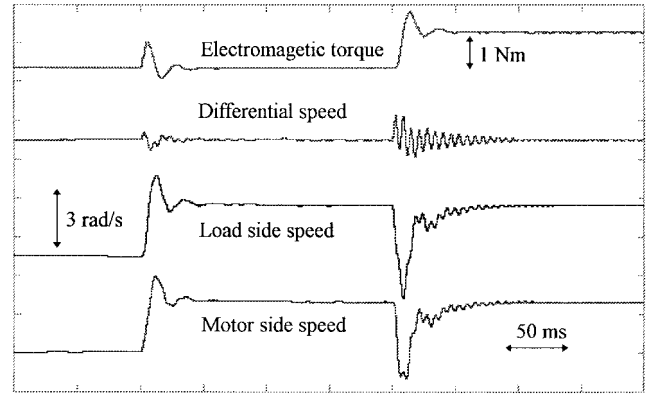

Fig. 8. Detuning of the FIR compensator. The dynamic response with 25% detuning of the time delay $T_{osc}/2$. The relative gain $G = 1.45$.

The dynamic response of the speed servo with flexible coupling and the FIR compensator is investigated by computer simulations. By virtue of the simulation results shown in Fig. 8, the proposed series compensator performs better than the notch filter (Fig. 5), in the presence of parameter uncertainty. The traces in Fig. 8 illustrate the case of 25% mismatch between $T_{osc}/2$ delay used by the series compensator and the actual half period of mechanical resonance. Notice that the robustness against parameter variations is immensely improved with respect to that of the notch compensator (Fig. 5). A detuned FIR compensator responds to the reference step with an insignificant increase of the overshoot, while the load step produces damped oscillations. At the same time, a detuned notch compensator exhibits the serious deterioration of closed-loop responses. Further investigations of the proposed antiresonant compensator are performed through systematic experiments.

IV. EXPERIMENTAL VERIFICATION

In the majority of practical cases, where the range of applicable gains is limited due to mechanical resonance, the problem reveals itself in the form of sustained oscillations. The audible noise and excessive tracking error reach unacceptable levels as gains are increased. This phenomenon depends upon the drive-train wear, temperature, control-loop bandwidth, offset of stator current controller, number of motor poles, shaft sensor characteristics, etc. It is the authors' belief that most of the aforementioned secondary effects are not modeled and covered by the simulations performed in Section III. Therefore, and for the sake of verifying experimentally the results from Section III, a set of measurements is performed on an experimental setup.

The setup is arranged according to the block diagram shown in Fig. 1 and consists of two synchronous permanent magnet servo motors connected by a flexible hollow shaft. The motor data are listed in Appendix II; torsional oscillations upon rapid load steps are found at 156 Hz, decaying to zero with the time constant of approximately 200 ms. Both motors are fed and controlled by a digital servoamplifier capable of both the torque- and the speed-control operating modes. The motor M1 (Fig. 1) is speed controlled, while the motor M2 is set in
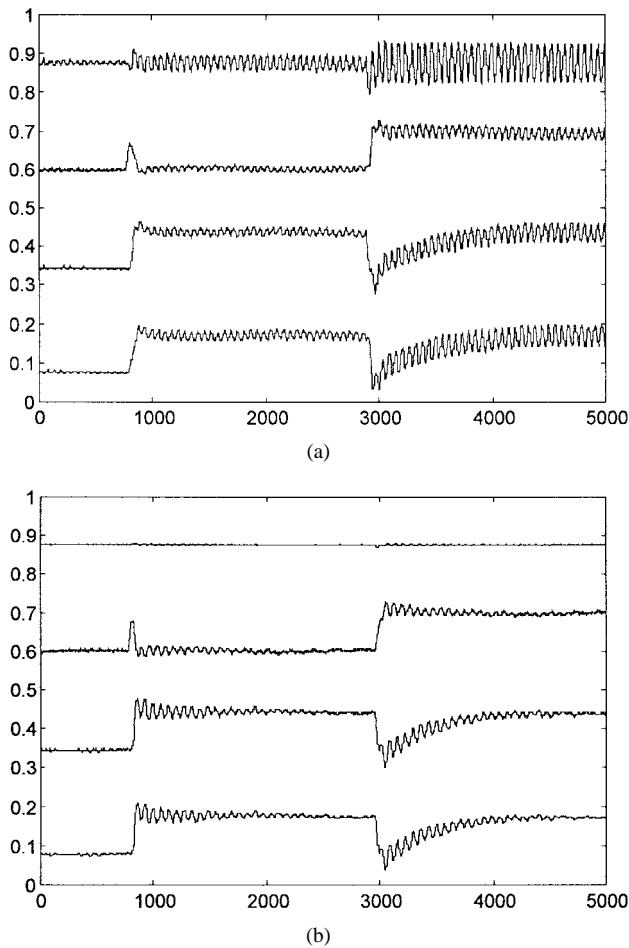
Fig. 9.   (a) Motor-side feedback. (b) Load-side feedback. The case with no series compensator and the loop gain $G = 100$. The experimental traces of the differential speed (the uppermost trace, 10 rad/s per div), the speed controller output or the torque reference (10 N·m per div), and load-side speed and the motor-side speed (the bottom trace, 10 rad/s per div).

the torque-control mode and used as a programmable load. The motors are equipped with electromagnetic resolvers. The resolver signals are decoded into the motor- and the load-side positions (θ_m and θ_l in Fig. 1) within the servoamplifier's control section. The R/D converter's bandwidth is 1 kHz and its resolution is 12 b. Having two shaft sensors at each end of the flexible coupling, it was possible to perform experiments with motor-side feedback and load-side feedback.

In order to decouple the mechanical resonance phenomena from speed and torque oscillations caused by the cogging torque of the permanent magnet motor, motor shafts are coupled, so as to minimize the sum of the cogging torques coming from the "motor side" and the "load side." For the same reason, experiments were performed at low speeds, keeping the measurement results free from cogging torque disturbances. The low-speed behavior is of great interest as far as the mechanical resonance is concerned, since the problem of sustained oscillations and instability are more acute, particularly at the zero speed.

Numerous experiments with various loop gains were performed. For the sake of brevity, a few experimental measurements are selected to illustrate the efficiency of the proposed

methods. In the experiments, the responses of three control structures with a conventional proportional integral (PI) controller were investigated. The first control structure did not include the antiresonance compensator. The second and third control structures include the notch series compensator and the proposed FIR compensator, respectively. The integral gain of the speed controller was kept at a low value, sufficient to make the drive track the reference input. At the same time, it is observed how the increase of the proportional gain sustains the mechanical resonance. The gain $G = 100$ of the DBM03 servo amplifier [25] corresponds to the relative gain $G_{max} = 1.45$ (Fig. 2).

In all traces included herein, the torque reference signal is obtained within the servoamplifier from the output of the speed controller. The internal torque signal is available at the output of the monitoring D/A converter built into the drive. Speed traces are obtained from the servoamplifier as well. For monitoring purposes, internal speed signals of 2S82 [20] R/D converters are filtered and presented at the output connectors of the drive. To minimize the impact of PWM-generated noise on monitoring signals, the filtering of all signals is performed within the servoamplifier unit by using a triple passive RC filter with 720-Hz cutoff frequency.

In Fig. 9, the experimental traces of the torque, motor speed, and load speed are obtained from systems with motor-side and load-side feedback compensated for by the series notch filter. Note that in Figs. 9–12, the uppermost traces represent the differential speed derived numerically by subtracting samples of motor- and load-side speed measuring signals. The motors are at a standstill at the beginning of the experiment. Subsequently, a small step in reference speed (100 r/min) is applied to the input of the speed controller. Finally, the load step of approximately 4 N·m is applied by setting up a negative torque reference for motor 2 held in the torque control mode (Fig. 1).

Under the same circumstances mentioned above, the systems compensated for by the cascade FIR digital filter were tested, and the experimental traces are shown in Fig. 10.

The robustness with respect to a parameter mismatch of the system with the notch series compensator is illustrated by the experimental traces shown in Fig. 11. In order to analyze the robust properties of the system with the FIR series compensator, the compensator central frequency has been detuned for 25%, and then the experimental traces shown in Fig. 12 were obtained. The traces in Figs. 11 and 12 verify the related results of simulation runs in Section III. Specifically, the experimental results prove the robustness of the proposed FIR series compensator that requires tuning of only one parameter and, therefore, it is well suited for use in an industrial environment.

V. CONCLUSION

Basic analytical considerations have been presented, along with a brief overview of methods for suppressing the torsional oscillations associated with high-performance servo drives in the frequency range above 100 Hz. Primarily, the cascade notch filtering is considered as a passive way of enhancing the performance of conventional speed controllers. Next, the
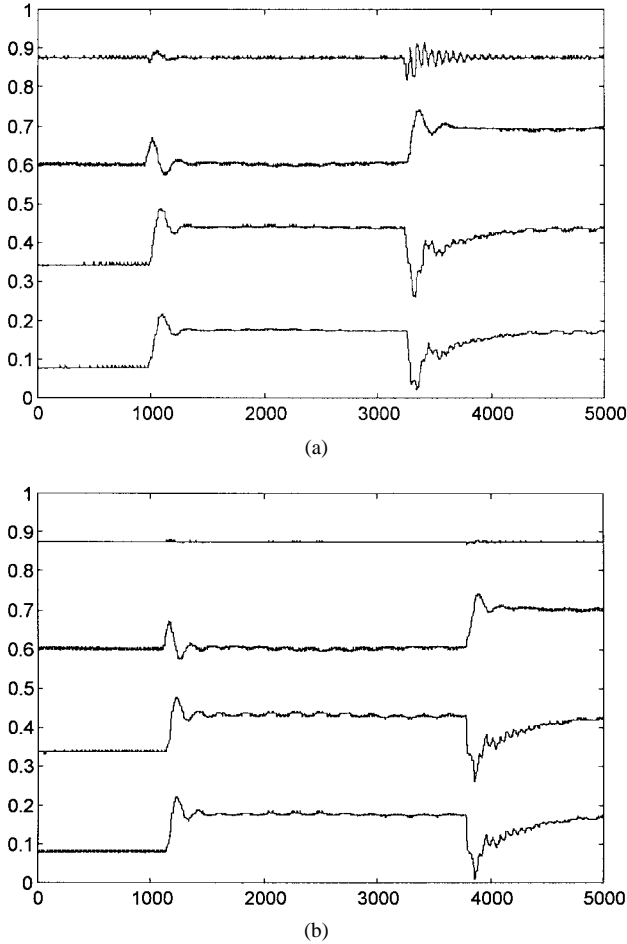
Fig. 10. (a) Motor-side feedback. (b) Load-side feedback. The case with FIR series compensator and the loop gain $G = 100$. The experimental traces of the differential speed (the uppermost trace, 10 rad/s per div), the speed controller output or the torque reference (10 N·m per div), and load-side speed and the motor-side speed (the bottom trace, 10 rad/s per div).
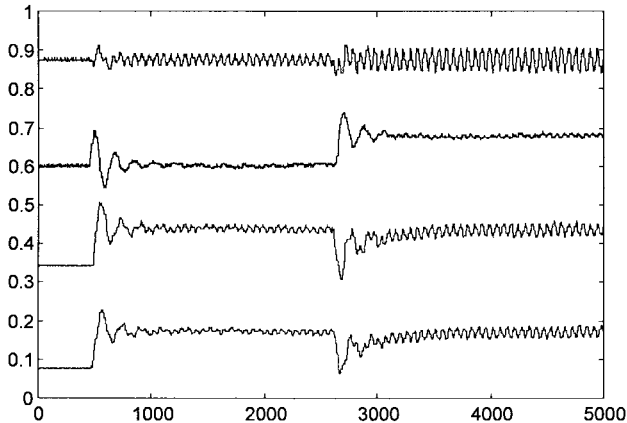

Fig. 11. Motor-side feedback with the notch series compensator. The loop gain $G = 100$ and 25% detuning of the notch central frequency. The experimental traces of the differential speed (the uppermost trace, 10 rad/s per div), the speed controller output or the torque reference (10 N·m per div), and load-side speed and the motor-side speed (the bottom trace, 10 rad/s per div).

analytical considerations and utilization of a simple single-parameter FIR digital filter for the suppression of resonance oscillations were presented, along with verification by means of computer simulations. Straightforward design guidelines for
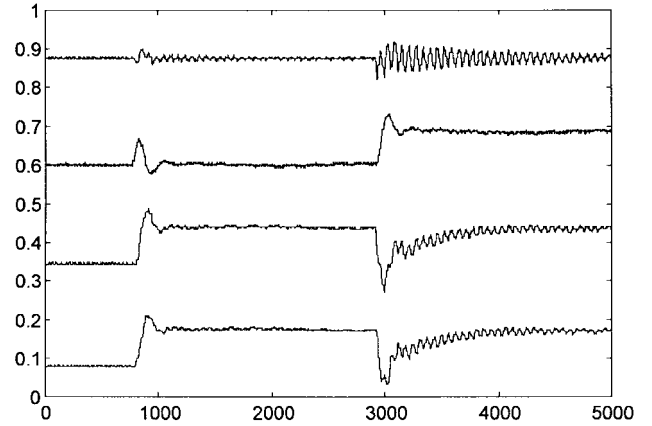

Fig. 12. Motor-side feedback with the FIR series compensator. The loop gain $G = 100$ and 25% detuning of the compensator's central frequency. The experimental traces of the differential speed (the uppermost trace, 10 rad/s per div), the speed controller output or the torque reference (10 N·m per div), and load-side speed and the motor-side speed (the bottom trace, 10 rad/s per div).

tuning the proposed compensator were given. The tuning does not require plant parameters, other than the half period of resonance frequency. Finally, brief explanations concerning the experimental setup are given. Measurement results are obtained on a test bed with elastically coupled 7 N·m synchronous servo motor and a mechanical resonance frequency of 160 Hz. The tests demonstrate the significant improvement of servo loop bandwidth and a notable enhancement of applicable loop gains. The experimental results are in agreement with the simulation runs and fully confirm the validity and efficiency of the proposed solutions.

APPENDIX I
DIGITAL IMPLEMENTATION OF THE NOTCH FILTER
WITHIN THE EXPERIMENTAL SETUP

The series notch filter compensator is built into the existing speed controller of the experimental setup. Since the digital section of the Vickers DBM03 servoamplifier uses a TMS320C14 processor, the notch filter is written in assembly language and linked with the existing code. The filter is coded according to discrete transfer function

$$W_{NF}(z) = \frac{K_3 z^2 - K_4 z K_5}{z^2 - K_1 z + K_2} \tag{A1}$$

with coefficients $K_1 \cdots K_5$ determined by (A2), where $\omega_p, \zeta_p,$ and ζ_z, denote, respectively, the notch filter center frequency, notch poles damping factor, and zeros damping factor. The filter width is determined by ζ_p, while the depth might be controlled through the ratio ζ_p/ζ_z. The parameters mentioned are set according to the resonant frequency and the viscous friction of the mechanical structure within the experimental setup:

$$\begin{aligned}
K_1 &= 2\exp(-\zeta_p\omega_p T)\cos(\omega_p T\sqrt{1-\zeta_p^2}) \\
K_2 &= \exp(-2\zeta_p\omega_p T) \\
K_3 &= \exp[-(\zeta_p - \zeta_z)\omega_p T] \\
K_4 &= \exp[-(\zeta_p + \zeta_z)\omega_p T],
\end{aligned} \tag{A2}$$

```
LAC      Reg_output       ;Reg_output = the output of the PI speed controller
ldpk     1                ;The notch filter variables X(n + 1), X(n), X(n − 1), Y(n + 1),
Sacl     Xnplus1          ;Y(n), and Y(n − 1) are located in page 1 of the DSP's
ZAC                       ;internal RAM
LT       Xnminus1
MPY      K5               ;The notch filter is implemented according to the formula
LTD      Xn
MPY      K4               ;Y(n + 1) = K1 * Y(n) − K2 * Y(n − 1) +
LTD      Xnplus1          ; + K3 * X(n + 1) - K4 * X(n) + K5 * X(n − 1)
MPY      K3
LTA      Ynminus1
MPY      K2
LTD      Yn
MPY      K1
APAC                      ;At this point accumulator keeps the filter output, it has to
;..............           ;be scaled and saved in Reg_Output torque reference.
LDPK     0
SACH     Reg_Output
```

The notch filter routine for the TMS320C14 DSP executes in 2.6 μs. Designed with 16-b representation of variables, the routine is written in assembly language and is shown at the top of the page.

APPENDIX II
EXPERIMENTAL SETUP DATA

The motors are FAST1M6030 synchronous permanent magnet servo motors with sinusoidal electromotive force and electromagnetic resolver attached to the shaft [25]. Two identical motors are connected via an elastic hollow shaft. The motors are independently controlled and used as the motor and the load (Fig. 1). The presence of the electromagnetic resolver at each end enables the testing of the motor- and the load-side feedback modes. The motor data are as follows:

$T_{\mathrm{nom}} = 5.7 \, \mathrm{N \cdot m};$

$T_{\mathrm{max}} = 24 \, \mathrm{N \cdot m};$

$\omega_{\mathrm{nom}} = 3000 \, \mathrm{r/min}$

$P_{\mathrm{nom}} = 1.49 \, \mathrm{kW};$

$p = 3;$

$J = 0.000\,620 \, \mathrm{kg \cdot m^2}$ (inertia of one motor including resolver);

$f_{\mathrm{res}} = 1.45 \, \mathrm{kHz}$ (shaft torsional resonant frequency with infinite load inertia).

The hollow shaft parameters are as follows:

$J_{\mathrm{sh}} = 0.000220 \, \mathrm{kg \cdot m^2}$ (the shaft and the coupling inertia);

$K_s = 350 \, \mathrm{N \cdot m/rad}$ (stiffness);

$K_v = 0.004 \, \mathrm{N \cdot m/rad}$ (viscous friction).

The servoamplifier is a DBM03 triple-axis servo amplifier.

REFERENCES

[1] T. Ohmae, T. Matsuda, M. Kanno, K. Saito, and T. Sukegawa, "A microprocessor-based motor speed regulator using fast-response state observer for reduction of torsional vibrations," *IEEE Trans. Ind. Applicat.*, vol. IA-23, pp. 863–871, Sept./Oct. 1987.

[2] S. Ozaki *et al.*, "A microprocessor-based dc motor drive with a state observer for impact drop suppression," in *Conf. Rec. IEEE-IAS Annu. Meeting*, Oct. 1983, pp. 771–775.

[3] G. Brandenburg and W. Walfermann, "State observers for multi motor drives in processing machines with continuous moving webs," in *EPE Conf. Rec.*, Oct. 1985, pp. 3.203–3.208.

[4] K. Sugiura and Y. Hori, "Vibration suppression in 2- and 3-mass system based on the feedback of imperfect derivative of the estimated torsional torque," *IEEE Trans. Ind. Electron.*, vol. 43, pp. 56–64, Feb. 1996.

[5] T. Hasegawa *et al.*, "A microcomputer-based motor drive system with simulator following control," in *Proc. IEEE IECON'86* 1986, vol. 1, pp. 41–47.

[6] M. Koyama and M. Yano, "Two degree of freedom speed controller using reference system model for motor drive," in *Conf. Rec. EPE'91*, 1991, pp. 208–212.

[7] K. Kaneko, K. Ohnishi *et al.*, "Accurate torque control for a geared DC motor based on an acceleration controller," in *Proc. IEEE IECON'92*, 1992, vol. 2, pp. 395–400.

[8] F. Profumo, M. Madlena, and G. Griva, "State variables controller design for vibrations suppression in electric vehicles," in *Conf. Rec. PESC'96*, 1996, pp. 1940–1947.

[9] R. Dhauadi, K. Kubo, and M. Tobise, "Analysis and compensation of speed drive systems with torsional loads," *IEEE Trans. Ind. Applicat.*, vol. 30, pp. 760–766, May/June 1994.

[10] J. K. Ji and S. K. Sul, "Kalman filter and LQ based speed controller for torsional vibration suppression in a 2-mass motor drive system," *IEEE Trans. Ind. Electron.*, vol. 42, pp. 564–571, Dec. 1995.

[11] K. Fujikawa *et al.*, "Robust and fast speed control for torsional system based on state-space method," in *Proc. IEEE IECON'91*, 1991, pp. 687–692.

[12] R. Dhauadi *et al.*, "Robust speed control of rolling mill drive systems using the loop transfer recovery design methodology," in *Proc. IEEE IECON'91*, 1991, pp. 555–560.

[13] R. Dhauadi *et al.*, "Two degree of freedom robust speed controller for high performance rolling mill drives," in *Conf. Rec. IEEE-IAS Annu. Meeting,* 1992, pp. 400–407.

[14] J. K. Ji, D. C. Lee, and S. K. Sul, "LQG based speed controller for torsional vibration suppression in 2-mass system," in *Proc. IEEE IECON'93*, 1993, pp. 1157–1162.

[15] J. Y. Hung, "Control of industrial robots that have transmission elasticity," *IEEE Trans. Ind. Electron.*, vol. 38, pp. 421–427, Dec. 1991.

[16] W. Leonhard, "Digital signal processing for trajectory control of a multi-axis robot with electrical servo drives," in *Proc. 15th IEEE IECON*, Philadelphia, PA, Nov. 1989, pp. 341–355.

[17] F. Ghorbel, J. Y. Hung, and M. W. Spong, "Adaptive control of flexible joint manipulators," *IEEE Contr. Syst. Mag.*, vol. 9, pp. 9–13, Dec. 1989.

[18] D. C. Hanselman, "Resolver signal requirement for high accuracy resolver to digital conversion," *IEEE Trans. Ind. Electron.*, vol. 37, pp. 556–561, Dec. 1990.

[19] S. T. Hung and J. C. Hung, "Digitally compensated resolvers," in *Proc. IECON'84*, Tokyo, Japan, 1984, pp. 625–627.

[20] *Design-in Reference Manual*, Analog Devices Inc., Norwood, MA, 1994, pp. 16.07–16.47.

[21] M. Uchiama and A. Konno, "Computed acceleration control for vibration suppression of flexible robot manipulators," in *Proc. 5th Int. Conf. Advanced Robotics*, Pisa, Italy, 1991, pp. 126–131.

[22] S. Colombi and T. Raimondi, "Compliance compensation in mechatronic systems," in *Proc. IEEE IECON'94*, 1994, pp. 946–951.

[23] S. Meshkat, "Digital control design for systems with resonance problem," in *Advanced Motion Control*, PCIM Reference Series in Power Electronics and Intelligent Motion. Ventura, CA: Intertec Communications, 1988, pp. 9–44.

[24] N. Sadegh and R. Horowitz, "Discrete time positioning adaptive control for systems with shaft flexibility," in *Advanced Motion Control*, PCIM Reference Series in Power Electronics and Intelligent Motion. Ventura, CA: Intertec Communications, 1988, pp. 171–175.

[25] "Fastact servo motors data sheets," Vickers Electrics, Genoa, Italy, 1994.

Milić R. Stojić (A'93) was born in Užice, Serbia (former Yugoslavia), in 1940. He received the B.S., M.S., and Ph.D. degrees from the Faculty of Electrical Engineering, University of Belgrade, Belgrade, Yugoslavia, in 1963, 1965, and 1967, respectively.

Since 1980, he has been a Full Professor with the Faculty of Electrical Engineering, University of Belgrade, teaching graduate and postgraduate courses in automatic control. In 1980, 1984, and 1988, he spent six months at the Physics Department, University of Birmingham, Birmingham, U.K., under the Cooperative Research Program. His scientific interests are in the sensitivity analysis of dynamic systems, system simulation, and microcomputer-based real-time control of electrical drives and industrial processes. He has published several books in Serbian, English, and Russian, and over 100 scientific papers. He is the author of *Continuous Control Systems*, 8th ed. (Belgrade, Yugoslavia: Science, 1996) and *Digital Control Systems*, 4th ed. (Belgrade, Yugoslavia: Science, 1994), written in Serbian, which are used as standard textbooks on automatic control at universities in Yugoslavia. He also developed two analog and digital student laboratories.

Prof. Stojić is the President of the Yugoslav Society of Electronics, Telecommunications, Computers, Automation, and Nuclear Engineering (ETRAN).

Slobodan N. Vukosavić (M'94) was born in Sarajevo, Bosnia-Hercegovina (formerly Yugoslavia), in 1962. He received the B.S., M.S., and Ph.D. degrees from the Faculty of Electrical Engineering, University of Belgrade, Belgrade, Yugoslavia, in 1985, 1987, and 1989, respectively.

In 1986, he joined the Nikola Tesla Institute, Belgrade, Yugoslavia, where he conducted research in the areas of static power converters and microcomputer-based control of electrical drives. Since 1989, he has been a Docent Professor with the Faculty of Electrical Engineering, University of Belgrade, teaching graduate and postgraduate courses in power electronics, control of electrical drives, and electrical traction. In 1988, he spent six months with the ESCD Laboratory, Emerson Electric, St. Louis, MO, in the Cooperative Research Program. Since October 1991, he has cooperated with Vickers Electrics, Genoa, Italy, under the Permanent Research Program, in the design and control of electrical drives for robots. His scientific interests are in the areas of system modeling and identification, microcomputer-based real-time control, power electronics, and rotating electrical machines design and control.